Numerical Identification of Design Parameters for Electromagnetic Forming

M. Stiemer[1*], Z. Nezhi[1], K. Rathjen[2], F. Zazai[1], M. Hagel[1], M. Rozgic[1]

[1] Institute of the Theory of Electrical Engineering, Helmut Schmidt University / University of the Federal Armed Forces Hamburg, Germany
[2] Institute of Fundamentals of Electrical Engineering, Helmut Schmidt University / University of the Federal Armed Forces Hamburg, Germany
*Corresponding author. Email: m.stiemer@hsu-hh.de

Abstract

In this work, approaches to the identification of high speed forming processes, whose simulation requires models from different parts of physics are discussed. Particularly emphasis is laid on situations in which it is possible to break off the coupling and to profit from partial solutions for the design of the whole process. Such situations arise if it is possible to select relevant features that allow for a stable transfer of information between the different models. Creating situations in which a sequential approach to a coupled problem is favourably possible requires a profound process understanding. As an example, an electromagnetic forming process is considered here. Approaches at identifying a coil geometry for electromagnetic forming are discussed in case of an exemplary case involving the definition of a suitable feature-list and the study of several methods to tackle the electromagnetic subproblem, including Nelder Mead Simplex Search, a combination of it with a neural network as surrogate model, and optimization via a neural network. These approaches are compared to each other, and quantitative results are given.

Keywords
Metal forming, Design optimization, Finite element method, Machine learning

1 Introduction

Many high speed forming processes are multi-physically coupled since the required momentum is transferred to the workpiece by mechanisms different from the established mechanical

transfer of momentum. This is, e.g., the case in electromagnetic forming (EMF), a process that is governed by the interaction of a large deformation thermo-elasto-viscoplastic material with a transient electro-magnetic field under magneto-quasistatic conditions (e.g., Unger, 2006). Although a precise prognosis of the process requires a fully coupled simulation, the identification of process designs that lead to a desired forming result can in some situations be split up in several steps: Just searching for a particular loading scenario that brings a mechanical structure in a desired state is usually not efficient, since the answer will lead in almost any case to a force distribution that cannot be provided by the process that is to be designed. But if instead a template for process forces that can be generated in a particular forming operation is at hand, this template can be filled by solving a purely mechanical inverse problem and then be used to identify the parameters related to those field that feed the required momentum into the material. In the case of EMF this means that the electro-magnetic field has to be determined for a loading situation that can indeed be realized by that technique. Here it becomes obvious that a deep understanding of the process, e.g., in the form that can be provided by approximative analytic models, or just some experience-based process knowledge is essential to be able to provide such a template. In this work we propose the selection of some relevant features of the process force which can be stored in a simple data format (a vector of manageable size) and for which simple conditions of feasibility can be derived. This vector can then be identified by a purely mechanical inverse problem and after that be used as target function for a purely electromagnetic (or, in case of other coupled processes, non-mechanical) inverse problem. The proposed paradigm of an effective feature selection is a typical step if a machine learning process is prepared, see, e.g., Roy et al. (2013). It is required in the input layer of the learning scheme and acts like an input filter that turns data into process relevant information. In this work we let both machine learning processes and mathematical optimization profit from feature selection and will tackle the corresponding inverse problems.

2 The Model Process

We will now define a simple electromagnetic forming process for which we will present and explain the framework just sketched before. Interest in this contact free high speed forming process stems among others from its potential of extending classical quasi-static forming limits (e.g., Kiliclar et al., 2016). Moreover, EMF processes are often less expensive than other processes and EMF can often easily be integrated in other process steps (see Psyk et al., 2011). As process parameters have, however, to be adjusted carefully in order to achieve a desired forming result, the interest in finding good designs for EMF is obvious.

2.1 The Process

We consider forming situations, in which a metallic work piece is formed by a nearby tool coil (see **Figure 1**). A capacitor bank is discharged into the tool coil which triggers a pulsed magnetic field in its environment. The work piece consists of aluminium (conductivity $\sigma_{\mathrm{Al}} =$

35 MS/m) and the coil of copper (conductivity $\sigma_{\mathrm{Cu}} = 58$ MS/m). The radius of the work piece amounts in all processes we consider in this work to 150 mm and its thickness to 1 mm. For the tool coil, three windings with a rectangular cross section are prescribed, which may vary in thickness and in the radii of the coils. The three inner and outer radii on some radius line and the height of the windings give 9 parameters that have to be identified during the design process (see below for the parameter ranges).

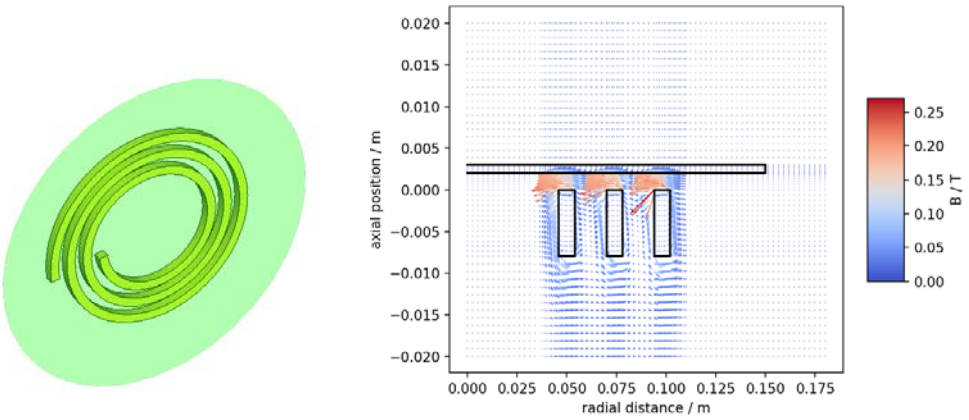

***Figure 1**: Example configuration: three-dimensional model for validation with CST Microwave Studio (left), flux density (right) for 30 kA after 10 µs computed by a fast axisymmetric FE-Python simulation.*

Due to induction phenomena on the molecular level the fast magnetic field can only slowly diffuse into the good conducting material, which evokes a strong spatial gradient of the magnetic field. By Ampère's law which yields under quasi-static conditions without Maxwell's correction, the curl of the magnetic field equals the current density in the material. As that the radial $\vec{\mathrm{e}}_\rho$-component strongly dominates under the sheet metal, the corresponding eddy currents possess azimuthal $\vec{\mathrm{e}}_\varphi$-direction and amount approximately to $\vec{J} = \frac{1}{\mu_0}\frac{\partial B_\rho}{\partial z}\vec{\mathrm{e}}_\varphi$. Consequently, $\vec{f} = \vec{J} \times \vec{B} = \frac{1}{\mu_0}\frac{\mathrm{d}B_\rho}{\mathrm{d}z} B_\rho \vec{\mathrm{e}}_z$ is a good approximation to the Lorentz force density, and integration over the thickness of the sheet metal yields the approximative equivalent pressure under the assumption of strong *B*-field localisation inside the work piece:

$$p = \frac{1}{2\mu_0}\left(B_{\rho,\mathrm{air}}^2 - B_{\rho,\mathrm{sheet}}^2\right) \approx \frac{B_{\rho,\mathrm{air}}^2}{2\mu_0} \approx 0.4 \times 10^6 \frac{\mathrm{N}}{(\mathrm{Tm})^2} \cdot B_{\rho,\mathrm{air}}^2 \qquad (1)$$

Hence, 1 T, sufficiently fast applied, gives simply speaking a forming pressure of 0.4 MPa and a flux density of 2 T correspondingly of 1.6 MPa.

2.2 Physical Description and Simplifications

As already indicated, relevant parameters of a complex thermo-mechanical model have to be represented by a certain number of features to be provided by the electromagnetic side.

While, in a full process identification, these features have to be determined by solving an inverse mechanical problem first, here we just set some values for the features that will be identified with suitable methods. Nevertheless, we will briefly sketch the mechanical model before we concentrate on the electromagnetic part of the process. On the mechanical side, energy is both elastically stored and dissipated. The split of both contributions depends at any instant on the state of deformation already assumed (in terms of stresses), the temperature, and – depending on the considered alloy – more or less on the forming velocity. As for metallic alloys plastic states usually correspond with large deformations, a large deformation elasto-viscoplastic material is relevant that has principally to account for the heating of the material. To be able to distinguish between possible and impossible forming procedures, a damage model is additionally be required. It can be implemented in a micromechanical motivated, thermodynamically consistent stressed based formulation as in Vladimirov et al. (2014) or less accurately via a phenomenological strain related formulation as in Taebi et al. (2011). Additionally, heat production and transfer have to be considered.

As the lengths of the electromagnetic waves related to the conditions under which EMF processes are driven, the magneto-quasistatic approximation applies, and displacement currents can be neglected. This leads to the decoupled system **Eq. 2** for the magnetic vector potential $\vec{A}$ and the electric scalar potential ϕ with permeability $\mu_\mathrm{r}\mu_0$ and conductivity μ_0 if a Coulomb gauge $\nabla \cdot \vec{A} = 0$ is imposed.

$$\frac{1}{\mu_0}\nabla \times \frac{1}{\mu_\mathrm{r}}\nabla \times \vec{A} + \sigma\frac{\partial \vec{A}}{\partial t} = \sigma\nabla\phi\,, \qquad \nabla \cdot (\sigma\nabla\phi) = 0\,, \qquad \nabla \cdot \vec{A} = 0 \tag{2}$$

The different physical fields are coupled in several ways. The most important phenomena are the Lorentz force between the electromagnetic and the mechanical system, the position of the work piece as a boundary condition to the electromagnetic system, thermal material softening and the change of the electrical conductivity due to heating. In principle it is important to consider the movement of the work piece in the physical process. However, as known from previous analysis (e.g., Stiemer et al., 2006, or Unger et al., 2006) the sheet metal does not move significantly in the first 10 µs of the process and a significant part of the energy transfer into the workpiece happens in this phase. Consequently, an analysis of this geometrically simple phase of the forming process is already interesting for its design. Later in the forming process, its dynamic will mainly be determined by inertial forces. It is already meaningful to consider the spatial distribution of the magnetic field in just one instant, say after 10 µs, since the shape of the electromagnetic field does only vary slightly and is basically only scaled. Hence, an optimization of the scaling can be done independently of the identification of a good spatial field distribution, since the first can always be adjusted in a second step by calibration of the triggering power in the capacitor bank.

2.3 Feature Selection

At first glance an optimum force profile determined by a purely mechanical simulation should provide good data for transferring relevant information from one subsystem to the other. However, such an approach contains severe problems. First, determining an optimum

force profile is an ill posed problem, and possible solutions will usually lack sufficient regularity. Consequently, mathematical regularization is required. Then, a high dimensional target value as a regularized, ideal force distribution may fail to correspond to a feasible force distribution, which is to be determined in the electromagnetic simulation. Hence, to overcome these problems, we construct here a low dimensional feature vector to exchange optimality information from the mechanical to the electromagnetic system. The feature vector is chosen based on simple physical insights in the forming process. Alternatively, an automated determination via convolutional neural networks (CNN) is an option (see below).

For the considered process, the metal plate is divided into a finite number of zones – below we will choose 5 just as an example. For each zone, the total force that should under optimum conditions be applied after 10 µs is determined. Such a distribution can be computed with the help of the algorithms discussed below, which can also be applied to a mechanical problem. A further legitimation for the proposed method stems from the observation that a formed geometry does not depend on the spatial variation of forces on a small scale. Only averages over larger areas are important.

3 Simulation with Different Accuracy and Cost

We present now three different methods to simulate the system considered as example.

3.1 Finite Element Simulation

To be able to perform many evaluations of a chosen objective (or cost) function, a finite element (FE) method has been implemented in Python. Bilinear elements on quads (Q1) have been used in an axisymmetric situation. Due to the simple geometry, an adapted meshing parallel to the axes is possible leading to a fast simulation for data generation (ca. 1000 simulations per hour for 2520 well distributed spatial degrees of freedom and 20 timesteps). In the adapted mesh, 7 points are introduced along the air gab between coil and sheet metal as well as between to coil windings or over the sheet. Time stepping is done by the backward Euler scheme with time steps of 0.5 µs and a GMRES solver is used for solving the resulting linear system. Stability with respect to the variation of discretization level and time step size has been studied. Forces are determined by integrating the Lorentz force density $\vec{f} = \vec{J} \times \vec{B} = \sigma_{\mathrm{Al}} \frac{\partial \vec{A}}{\partial t} \times \left(\nabla \times \vec{A}\right)$ obtained from the magnetic vector potential first over the thickness with the summed trapezoidal rule (thus obtaining the equivalent pressure) and later over the 5 radial zones. To be able to work in an axisymmetric context, the coil is replaced by a system of 3 rings with corresponding cross sections. Each ring is cut at an azimuthal position $\varphi = 0$ and one cut surface is virtually connected with the other surface of the preceding ring (or with a terminal connection), while the other is connected with the counterpart on the following ring (or with a terminal connection). A solution of the scalar potential equation is first determined from a guess of the potential current and taken as right-hand side in the eddy current equation. Then it is rescaled so that the total current (sum of potential and eddy current) amounts to a prescribed value. The spatial distribution of the

potential current density is determined such that all crosscuts through any winding are on the same potential and the current density scales according to the changing resistance due to a different length of the current paths at different radial position (see Stiemer et al., 2006).

3.2 Validation with CST Microwave Studio

The finite element simulation has been validated by a highly accurate simulation with the commercial program CST Microwave studio from Dassault Systèmes. Using more than a million spatial degrees of freedom, a computing time of 10 h has been required to determine a reference solution. In **Figure 2**, the dominant component of the magnetic fields along the radial axis of the CST result and the result of the fast FE-simulation after 25 µs process time are compared to each other. The field is triggered such that the total current has the shape of a double exponential pulse with rise time of 10 µs, fall time 100 µs , total duration of 100 µs, and maximum of 30 kA. Later, however, for the inverse identification of the feature vector, a damped sinus has been chosen for the course of the current. All geometric parameters are chosen as given before apart from the airgap between tool coil and workpiece. It is 1 mm in the identification computations and 2 mm in the validation process.

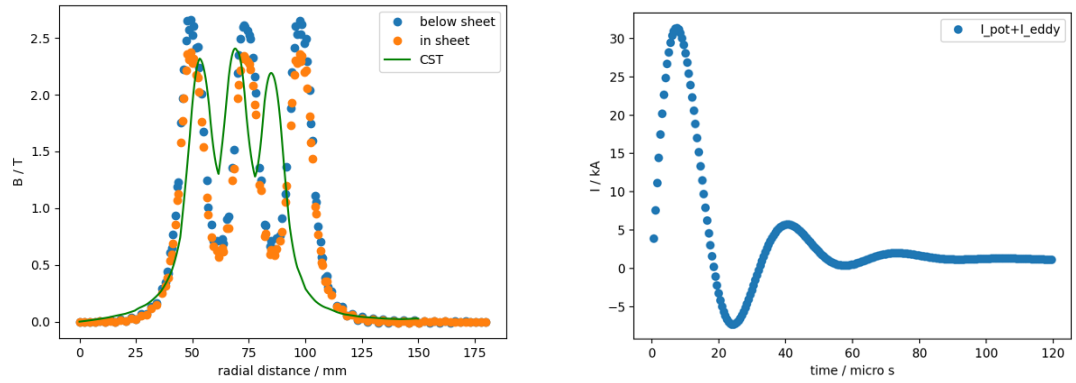

***Figure 2**: Scaled magnetic flux density (left, below and in the sheet after 25 µs triggered by a double exponential pulse), current distribution (right) for feature identification.*

Unfortunately, the values computed with the fast FE method remain by a factor of 2π below the CST-values. The computed forces behave correspondingly. A possible cause of this problem may lie in the partition of potential- and eddy currents. It does, on the other hand, not affect the point of study in the present work: The main concern is an identification of a good spatial field distribution. Whenever such a distribution has been found, scaling via power supply (capacitor bank) is still possible. Slight spatial deviations in Figure 2 are probably due to the CST model being fully 3-dimensional.

3.3 Neural Networks as Surrogate Models

If a large amount of learning data is at disposal, difficult problems with no clear structure can be tackled with machine learning techniques. Among these artificial neural networks

belong to the most prominent methods. Authors like and Woo et al. (2018) or Lee et al. (2018) use them to identify parameters for high speed forming processes, Lee et al. (2018) examined even electromagnetic forming. In this work, a NN is used to learn the prediction of the FE model so that it can later be used as faster surrogate model in optimization. In addition, we have it also used to solve the feature identification problem itself, i.e., by identifying electromagnetic process parameters that lead to the desired features.

4 Numerical Examples

The previously discussed selected features are now specified by several values which in practical applications will be determined by an inverse problem for a mechanical simulation framework. Thus, those feature values are computed, which will lead to an optimum forming result. This important step is not contained in this paper. However, the corresponding inverse problems can be tackled with the same methods as applied here for the electromagnetic system. The feature vector contains the following 5 areas, each corresponding to a part of the plate confined to a particular radial zone (see **Table 1**).

Radial Zone	Z1	Z2	Z3	Z4	Z5
Limiting radii	$0 \leq \rho \leq 30$ mm	$30 \leq \rho \leq 60$ mm	$60 \leq \rho \leq 90$ mm	$90 \leq \rho \leq 120$ mm	$120 \leq \rho \leq 150$ mm
Required force	0 kN	5 kN	7 kN	2 kN	0 kN

***Table 1**: Radial zones the total force transmitted to the workpiece is computed for.*

For the 9 parameters to be identified to obtain the prescribed feature vector, the following restrictions are implemented:

$$\begin{aligned} &5 \text{ mm} \leq u_0 < o_0 < u_1 < o_1 < u_2 < o_2 \leq 130 \text{ mm}, \\ &5 \text{ mm} \leq b_0, b_1, b_2 \leq 11 \text{ mm} \end{aligned} \tag{3}$$

Here (u_k) are the inner, $(\boldsymbol{o_k})$ the outer radii, and $(\boldsymbol{b_k})$ the heights of the three windings.

4.1 Use of a Neural Networks as Surrogate Model

A neural network consisting of an input layer of 9 cells (size of the parameter vector) and an output layer of 5 cells (size of the feature vector) has been trained with 10000 data points. The quality of the prognosis for unknown test data is depicted in **Figure 3** (left) and compared to that of the inverse problem (right) from Section 4.3. All NN employed in this work have been implemented by Keras and the TensorFlow library of Python 3.

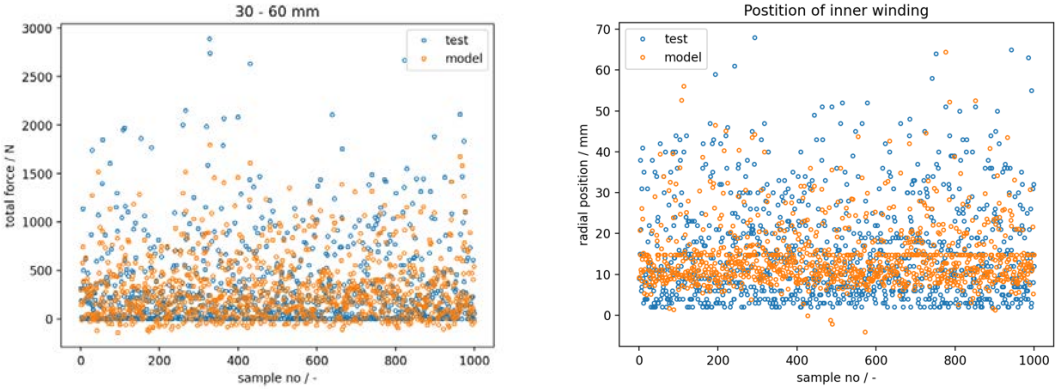

***Figure 3**: Success of the predicted force in zone Z2 (surrogate model, left) and for the position of the inner winding (inverse problem, right).*

Between input and output layer 3 hidden layers with first 64 neurons and then 128 each have been placed. The activation function was always the rectified linear unit activation function (relu) and a mean squared error (mse) has been taken as cost function. The regression for computing the internal weights of the neurons was carried out with the Adam method. For about 66% of unknown parameters the prognosis was sufficiently usable. After that, the model was employed to compute the objective function in the Nelder Mead algorithm instead of the finite element model, which is much faster than using the FE method. The obtained results stayed stable when algorithmic parameters were slightly changed (see below).

4.2 Optimization with Nelder Mead Method

Within 100 iterations the Nelder Mead method arrived successfully close to the feature vector (0.00 kN, 4.97 kN, 7.00 kN, 2.00 kN, 0.00 kN) with a mean squared deviation of less than 0.0025 kN. The target function was simulated via finite element simulation as described in Section 4.1. The optimization took approximately half an hour.

Replacing the finite element-based target function by a surrogate model according to Section 4.1 did not lead to good results. The optimization time was drastically reduced to some seconds. Although the mean squared error was reduced to a bit more than 1/630 of its starting value, no reasonable results could be obtained. In contrast to the FE target function, the Nelder Mead algorithm showed the tendency to choose parameters far away from reasonable values. In an extended approach it is now planned to filter out non-compliant values and to work with combinations of a surrogate model and an exact FE-based model, such that the fraction of FE-based model evaluations increases continuously. With each FE- model evaluation, the surrogate model can be further trained such that its accuracy is also augmented. A larger NN (128 neurons per layer instead of 64) did not change the findings.

4.3 Treating an Inverse Problem by a Neural Network

Next, we treat the identification problem for the feature vector just by changing the role of the parameters and the feature vector. Consequently, instances of the latter are now considered as input data, while approximations to the corresponding parameters created by a model are the output. The aim is to obtain a scheme to determine a suitable parameter vector for a given feature vector, i.e., to solve an inverse problem to the given model. While such an inverse problem is generally not uniquely solvable, we may profit from a bias in the learning data: the data pairs provided as learning data stem from reasonable forward problems. When the neural network learns from these data, it is likely that the NN only produces reasonable solutions during the test- and application phase. In fact, we got an accuracy of 98% on an unknown training set (see Figure 3, right). Remarkably, with the feature extraction performed here, the inverse problem (finding parameters that lead to the force distribution searched for) was easier to learn for the NN than the original problem. However, as for the direct surrogate model, compliance of the proposed parameters will have to be enforced in further developments.

4.4 Automatic Feature Extraction

Feature extraction is a common process in machine learning. It is usually not explicitly referred to in mathematical optimization, where the optimization problem is formally described by constraints and an objective function. However, the effect of a feature extraction enters into a mathematical framework often via regularization of ill-posed problems. Here, we concentrate on feature extraction to render the approach to the parameter identification problem via separation into partial problems feasible. In contrast to a manual, experience-based feature selection, this task could also be done automatically by a CNN (see, e.g., Albawi et al., 2017). This can be used as an encoder in front of a fully connected multi-layered network. Complex data as, e.g., the pressure distribution over the surface of a workpiece, can be processed by the CNN and rendered into a meaningful low dimensional structure to be used as input to the full layers of the network. The other way round, a conjugated network can act as a decoder to restore complex data from the output of the fully connected layers.

5 Conclusion and Perspectives

In this paper approaches at dividing a coupled problem in a series of identification problems, which are easier to solve than the whole problem, are discussed. Some part of a comprehensive proposal for EMF is implemented and tested. The method relies on project knowledge and a physical insight into it. This is the basis on which important features can be identified. To solve the identification problems, a fast FE method together with the Nelder Meat simplex search performed well. Also, the application of the NN to the solution of the inverse problem worked surprisingly well. The next step to do will be the identification of a feature map for EMF by a mechanical simulation (e.g., LS-Dyna) and a validation of the complete identified parameter set in the end. Moreover, different designs of optimization algorithms

will be tested. It seems to be of particular interest to reduce computing power by introducing surrogate models in a controlled way up to a reasonable point. This is related to impulse forming, since process knowledge will also play an important role in the design of such hybrid identification schemes.

In the long term, it is expected that all kind of technological devices will rely on a digital twin, who already organizes parts of the design process before a device is produced. In such a context, optimization algorithm would play an important role, both in the classical form as well as in form of machine learning processes. The latter have become an alternative due to the high availability of large amounts of data. In engineering, however, data are much more expensive to obtain than in classical areas of data analytics. Here error-controlled simulation will play an important role as well as consequent data recycling, i.e., collecting of all types of data that occur. Design problems do not always require accurate models to identify good configurations. Accordingly, various types of models may coexist and may be used as different tools in a toolbox.

References

Albawi, S., Mohammed, T.A., Al-Zawi, S., 2017. Understanding of a convolutional neural network. In: Int. Conf. on Engineering and Technology (ICET) 2017, IEEE, pp. 1-6.

Kiliclar, Y., Demir, O.K., Engelhardt, M., Rozgič, M., Vladimirov, I.N., Wulfinghoff, S., Weddeling, C., Gies, S., Klose, C., Reese, S., Tekkaya, A.E., Maier, H.J., Stiemer, M., 2016. *Experimental and numerical investigation of increased formability in combined quasi-static and high-speed forming processes.* J. Mater. Process. Technol. 237, pp. 254-269.

Luca, D, 2015. *Neural networks for parameters prediction of an electromagnetic forming process of FeP04 steel sheets.* Int. J. Adv. Manuf. Technol. 80, pp. 689-697.

Lee, S., Kang, B.S., Lee, K., 2018. *Comparative Study on Surrogate Modeling Methods for Rapid Electromagnetic Forming Analysis.* Trans. Mater. Process. 27 (1), pp. 28-36.

Psyk, V., Risch, D., Kinsey, B.L., Tekkaya, A.E., Kleiner, M., 2011. *Electromagnetic forming – A review*. J. Mater. Process. Technol. 211 (5): 787-829.

Roy, A., Mackin, P. D., Mukhopadhyay, S, 2013. *Methods for pattern selection, class-specific feature selection and classification for automated learning.* Neural Networks 41, pp. 113-129.

Stiemer, M., Unger, J., Svendsen, B., Blum, H., 2006. *Algorithmic formulation and numerical implementation of coupled electromagnetic-inelastic continuum models for electromagnetic metal forming.* Int. J. Numer. Methods Eng. 68 (13), pp. 1301-1328.

Taebi, F., Demir, O.K., Stiemer, M., Psyk, V., Kwiatkowski, L., Brosius, A., Blum, H., Tekkaya, A.E., 2012. *Dynamic forming limits and numerical optimization of combined quasi-static and impulse metal forming.* Comput. Mater. Sci. 54, pp. 293-302.

Unger, J., Stiemer, M., Svendsen, B., Blum, H., 2006. *Multifield modeling of electromagnetic metal forming processes.* J. Mater. Process. Technol. 177 (1-3), pp. 270-273.

Vladimirov, I.N., Pietryga, M.P., Kiliclar, Y., Tini, V., Reese, S., 2014. *Failure modelling in metal forming by means of an anisotropic hyperelastic-plasticity model with damage.* Int. J. Damage Mech. 23, pp. 1096-1132.

Woo, M.A., Lee, S.M., Lee, K.H., Song, W.J., Kim, J., 2018. *Application of an Artificial Neural Network Model to Obtain Constitutive Equation Parameters of Materials in High Speed Forming Process.* Trans. Mater. Process. 27 (6), pp. 331-338.